May 9-12
Kyoto-Japan
2017

2nd International Workshop on
Sediment Bypass Tunnels

Downstream morphological effects of SBT releases: 1D numerical study and preliminary LiDAR data analysis

Matteo Facchini, Annunziato Siviglia and Robert M. Boes

Abstract

Sediment bypass tunnels (SBTs) are built with the twofold aim of reducing reservoir sedimentation and restoring sediment and water regimes in the downstream reach. The conveyance of water and sediment through SBTs has the potential to cause downstream morphodynamic changes, which have so far been poorly investigated. The main goal of this work is to quantify downstream morphological effects of SBT releases. This will be achieved conducting a numerical study on an idealized but still realistic situation and a field data analysis. First, assuming that the SBT transport capacity is larger than the one of the upstream river reach, we identify realistic SBT-release scenarios in terms of water and sediment discharges being released from the SBT and the dam to the downstream reach. Second, we carry out a numerical study for the quantification of the impacts of SBT operations in terms of bed level and surface sediment grain size changes. Third, we analyze the effect of the SBT releases that occurred in 2014 and 2016 at the Albula River, through a comparison of data collected during two LiDAR surveys carried out after SBT releases. Numerical results show that i) the smaller the water discharge released from the SBT, the steeper the riverbed becomes; ii) if the SBT is delivering sediment and water to the downstream reach, the riverbed grain size distribution (GSD) tends to be close to unarmored conditions, with slight changes for different release conditions. Considering a reduced SBT-efficiency (i.e. only a part of the sediment being transported in the upstream reach is entering the SBT), the described trends do not change but the equilibrium riverbed slope becomes smaller, with some release conditions causing the downstream slope to be smaller than the upstream one. Finally, from the comparison of cross-sections obtained from the points measured with two LiDAR surveys, we observe a significant depositional trend in the river reach downstream of the Solis SBT (Canton Grisons, Switzerland), as can be inferred from the numerical simulations.

Keywords: sediment bypass tunnels, gravel bed-rivers, numerical modeling, grain sorting

1 Introduction

By interrupting natural water flow and sediment regimes, dams modify river morphology with different consequences upstream and downstream of the barrage. Upstream, they confine reservoirs, thus causing the formation and development of an aggradation body

inside the reservoir, which reduces the reservoir storage capacity (Morris and Fan 1998). In the downstream reach, reduced water flow and interruption of sediment supply induce mainly channel narrowing and degradation together with coarsening of the riverbed surface (e.g. Williams and Wolman 1984). This results often in armoring of the riverbed surface, i.e. due to selective transport by size fraction the riverbed surface becomes coarser than the bedload to a great extent. Static-armoring of riverbed surfaces leads to vanishing or near-vanishing bedload transport, while mobile-armoring of riverbed surfaces allows for bedload transport of the finer fractions. If all the grain sizes present on the riverbed surface are represented in the bedload with the same fraction as on the riverbed surface, the river is in unarmored condition. That is the riverbed surface has exactly the same grain size distribution (GSD) as the bedload.

To counteract reservoir sedimentation, many techniques have been implemented at dam sites, and can be grouped in three main categories: i) sediment yield reduction, ii) sediment routing, and iii) sediment removal (Sumi *et al.* 2004). Sediment routing techniques have been proven to have positive effects in countering reservoir sedimentation (e.g. Sumi *et al.* 2004), but whether or not they can act as a mean for sediment replenishment below dam is still an open research question. On the contrary, gravel augmentation, i.e. the artificial addition of gravel to a stream, has been successfully used by hydraulic engineers, fluvial geomorphologists, and fishery biologists as a mean to mitigate sediment paucity below dams (e.g. Bunte 2004). Moreover, where sediment augmentations were difficult to perform, water releases have been used as an alternative to reactivate sediment transport and enhance habitat quality downstream of dams (e.g. Robinson *et al.* 2004).

Among the techniques used to route sediments around dams, SBTs have proven to be effective at conveying both bedload and suspended load to the downstream river reach (Sumi *et al.* 2004), but the effects of SBT releases on the downstream morphology are still poorly investigated. Moreover, the dynamic induced by sediment-laden waters released by SBTs downstream of dams is complicated by the interplay between water and sediment.

The final goal of this work is to quantify the morphological changes in terms of riverbed slope and grain size distribution (GSD) induced by realistic SBT operations. First, we identify realistic SBT-release scenarios. Second, we carry out a numerical study aiming at quantifying the morphological effects of SBT-releases. Eventually, we study the actual morphological changes occurred between two large SBT releases at the Solis dam (Canton Grisons, Switzerland) in 2014 and 2016.

2 SBT-release scenarios

Possible SBT-release scenarios are defined in terms of water and sediment discharge being conveyed through the SBT to the downstream reach. They are obtained starting

from the observation that, to properly work, a SBT must have a higher sediment transport capacity than the river flowing in the reservoir. Therefore, given the slope and the GSD of the upstream river reach, the relationship between the water Q_w and the bedload discharge Q_b (i.e. the bedload rating curve, BRC) can be calculated for the upstream (index u) river reach (BRC_u) and the SBT (BRC_{SBT}), corresponding to the solid red and blue lines in Fig. 1. We consider the SBT and dam outlets as the mean to reestablish water and sediment continuity at dams. That is, what is transported in the upstream river reach is then conveyed through the SBT and dam outlets, acting as an upstream boundary condition to the downstream river reach.

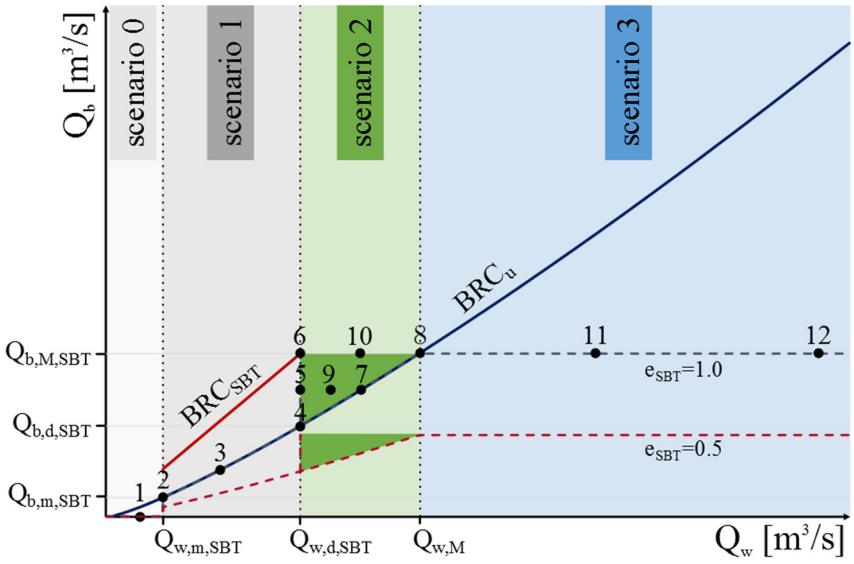

Figure 1: Bedload rating curves (BRC) for the SBT (red) and the upstream river reach flowing into the reservoir (blue); black dots and numbers refer to numerical runs; the dashed lines represent what is conveyed to the downstream reach, considering the SBT-release efficiency e_{SBT}=1.0 (grey) and e_{SBT}=0.5 (red), i.e. the SBT operating conditions.

In most of the cases, bedload and riverbed surface GSDs of rivers at which SBTs are built are composed of a mixture of sand and gravel. To take into account the effect that sand has on coarser grains, we compute the BRC_u adopting the Wilcock and Crowe (2003) sediment transport formula, while for the SBT we adopt the Smart and Jaeggi (1983) formula as suggested by Albayrak *et al.* (2016) and Boes *et al.* (2017). SBTs are usually designed (index d) according to a given water (index w) discharge value $Q_{w,d,SBT}$. On the BRC_{SBT} curve, $Q_{w,d,SBT}$ identifies the maximum (index M) bedload (index b) discharge that can be transported through the SBT ($Q_{b,M,SBT}$). The Q_w needed for carrying the maximum SBT bedload discharge in the upstream reach is termed $Q_{w,M}$. On the BRC_{SBT} curve, it is also possible to identify the minimum (index m) value of Q_w for which the SBT is first put in operation ($Q_{w,m,SBT}$), together with the corresponding minimum bedload discharge transported through the tunnel ($Q_{b,m,SBT}$). Then, we can identify four possible

scenarios in terms of water and bedload discharges released by the SBT to the downstream river reach (see Fig. 1):

- scenario 0 (very small events, i.e. $Q_w < Q_{w,m,SBT}$): the SBT is not operated and bedload carried by the upstream river, once the threshold of motion is exceeded, is all stored in the reservoir;
- scenario 1 ($Q_{w,m,SBT} \leq Q_w \leq Q_{w,d,SBT}$): the entire amount of sediment coming from upstream is diverted downstream through the SBT and the possible SBT operations are identified by the points 2, 3, and 4 lying on the BRC_u curve;
- scenario 2 ($Q_{w,d,SBT} < Q_w \leq Q_{w,M}$): the water and bedload discharges being delivered to the downstream reach range between the SBT design discharges (i.e. $Q_{w,d,SBT}$ and $Q_{b,d,SBT}$) and the maximum discharges possible (i.e. $Q_{w,M}$ and $Q_{b,M,SBT}$). This gives rise to two extreme situations: the first occurs when the water discharge fed to the downstream reach is kept constant, i.e. $Q_w = Q_{w,d,SBT}$, and the surplus, i.e. Q_w-$Q_{w,d,SBT,}$ is stored inside the reservoir, while the bedload discharge ranges between the design value and the maximum one, i.e. $Q_{b,d,SBT} \leq Q_b \leq Q_{b,M,SBT}$ (points 4, 5, and 6 in Fig. 1). The second occurs when water and bedload discharges fed to the downstream reach range both between the design and the maximum value, i.e. $Q_{w,d,SBT} < Q_w \leq Q_{w,M}$ and $Q_{b,d,SBT} < Q_b \leq Q_{b,M,SBT}$ (points 4, 7, and 8 in Fig. 1). Between these two situations a number of other release scenarios is possible, like e.g. points 9 and 10, or more generally all the points lying inside the green area bounded by points 4, 6, and 8 in Fig. 1;
- scenario 3 (very large floods, i.e. $Q_w > Q_{w,M}$): the bedload discharge fed to the downstream reach is constant and equal to the maximum transport capacity of the SBT (i.e. $Q_{b,M,SBT}$) and the water discharge increases above $Q_{w,M}$ needed to carry $Q_{b,M,SBT}$ in the upstream river reach, since extra water not flowing through the SBT is released from the dam.

The scenarios described above are obtained assuming that SBTs always work with an SBT-efficiency of $e_{SBT} = 1.0$. That is, sediment being transported in the upstream reach is conveyed entirely through the SBT. Literature studies suggest that SBTs usually do not carry all the bedload material coming from upstream, i.e. SBTs are generally characterized by $e_{SBT} < 1.0$, and it comes across that e_{SBT} decreases with increasing incoming water discharge (e.g. De Cesare *et al.* 2015). Auel *et al.* (2016) report e_{SBT}–values of 0.77 and 0.94 for the Japanese SBTs Asahi and Nunobiki, respectively, where total sediment flows are considered. For Nunobiki SBT, all coarse sediments enter the SBT even for floods with $Q_w > Q_{w,d,SBT}$ (Auel *et al.* 2016), i.e. $e_{SBT} \rightarrow 1$ regarding bedload. However, in addition to fully efficient SBTs we also consider reduced e_{SBT}–values in our runs by halving the bedload discharge Q_b being carried by the SBT, i.e. considering $e_{SBT} = 0.5$ (see dashed red line in Fig. 1).

3 Downstream morphological effects: numerical study

To quantify the downstream changes in riverbed slope and GSD due to SBT-releases, we run numerical simulations with BASEMENT (Vetsch *et al.* 2017). We consider a simplified configuration, i.e. a straight channel with rectangular cross-section 15 m wide, non-erodible walls and constant slope of 0.015. At the upstream boundary a hydrograph and a sedimentograph are imposed according to the possible SBT-release scenarios. The values relative to the hydro- and sedimentograph peaks are the ones represented by the numbered dots in Fig. 1. Water and sediment discharges vary in parallel in time and are cycled until mobile-bed equilibrium is attained. At mobile-bed equilibrium, riverbed slope and GSD are oscillating in time around defined values, due to varying water and bedload discharges at the upstream boundary. A bimodal GSD typical of a gravel bed river is fed at the upstream boundary, having 25% of sand content, geometric mean size $d_{s,g}$ = 16.22 mm and geometric standard deviation σ_g = 7.27 mm. The simplified geometry, the hydro- and the sedimentograph, and the GSD used for the numerical runs resemble the geometrical characteristics of the river reach downstream of the Solis SBT (Canton of Grisons, Switzerland), the hydro- and sedimentograph shape and duration of the August 13, 2014 flood, and the GSD of the material sampled in the vicinity of the SBT inlet structure (see e.g. Facchini *et al.* 2015).

Numerical results are given in Fig. 2 and Fig. 3, where a non-dimensional water discharge relative to the SBT design discharge, i.e. $Q^*_w = Q_w/Q_{w,d,SBT}$, is shown on the abscissa. The results on the ordinate are presented in terms of non-dimensional geometric mean size of the riverbed surface $d^*_{s,g} = d_{s,g}/d_{s,g,f}$, where $d_{s,g}$ and $d_{s,g,f}$ are the geometric mean sizes at equilibrium and of the feeding, and non-dimensional riverbed slope S^*, defined as the ratio between the final downstream equilibrium river slope S and the reference upstream slope S_{ref}, i.e. $S^* = S/S_{ref}$. The reference values we chose for $d^*_{s,g}$ and S^*, i.e. $d_{s,g,f}$ and S_{ref}, represent the target values to evaluate the effectiveness of SBT in reestablishing pre-dam conditions in the downstream reach. That is, if the goal of SBTs is reestablishing water and sediment continuity at dams, S^* = 1.0 and $d^*_{s,g}$ = 1.0 represent the situation where the downstream river reach has the same slope and riverbed surface GSD of the upstream reach. Since usually downstream reaches have lower slopes than upstream ones (e.g. Schmidt and Wilcock 2008), we can consider that $S^* > 1.0$ indicates a deposition trend, while $S^* < 1.0$ indicates an erosion trend. Moreover, the closer the riverbed surface GSD is to that of the feeding material (i.e. the closer $d^*_{s,g}$ is to 1.0), the less armored the riverbed surface (Parker and Sutherland 1990). Unarmored conditions are a favorable outcome of sediment augmentation plans below dams, since they are the opposite of what results from river damming, i.e. riverbed armoring (e.g. Williams and Wolman 1984).

Results show that final configurations have a low armoring degree of the riverbed surface, i.e. $d^*_{s,g}$ tends to 1.0 since $d_{s,g}$ tends to $d_{s,g,f}$, the higher the feeding rate. In fact, runs 6, 10, 8, 11, and 12 (connected by the dot-dashed red and blue lines in Fig. 2) have the same

equilibrium $d^*_{s,g}$, which is around 1.5 for e_{SBT} = 1.0 (blue dots in Fig. 2) and around 1.6 for e_{SBT} = 0.5 (red diamonds in Fig. 2). The riverbed GSDs at mobile-equilibrium are thus slightly different among the possible scenarios, with slightly coarser riverbeds in case of reduced e_{SBT}. Irrespective of e_{SBT}, in case of very small floods (scenario 0, run 1), the equilibrium riverbed results to be armored ($d^*_{s,g}$ > 6.0) because only water is delivered downstream, the riverbed is eroded, the transport capacity decreases and only finer grains are transported, leaving the coarser particles on the riverbed. However, the resulting GSD for run 1 is finer than the one of the static armor which corresponds to $d^*_{s,g}$ = 10.6. This is representative of the GSD obtained with the formula proposed by Parker and Sutherland (1990), which links the riverbed GSD to the transported GSD starting from the assumption that with a static armor no sediment transport takes place.

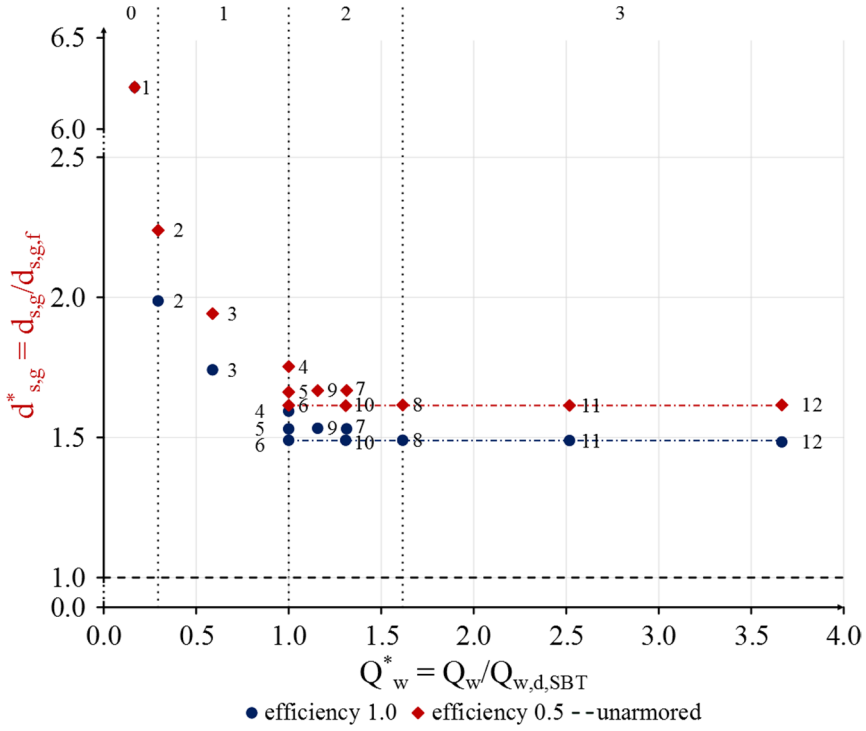

Figure 2: Results at mobile-bed equilibrium concerning bedload GSD represented by the non-dimensional geometric mean size $d^*_{s,g}$.

Concerning riverbed slopes at mobile-bed equilibrium, the results show that with e_{SBT} = 1.0, if the SBT is delivering water and sediment to the downstream reach (runs 2 to 12), they become steeper than the upstream slope, which we use as a reference (black dashed line in Fig. 3). On the contrary, assuming e_{SBT} = 0.5 results in several runs with a riverbed slope at mobile-bed equilibrium close to the upstream one (e.g. runs 3, 4, 7 and 8 in Fig. 3), and two cases (runs 11 and 12 in Fig. 3) in which the large flood water discharge results in riverbed slopes lower than the upstream one. For moderate SBT-efficiency, the downstream reach will thus be less steep than the upstream one in the case of large floods, but its riverbed surface composition will nevertheless be close to the feeding one, i.e. the

armoring degree will be far from the static armor. Regardless of e_{SBT} if the downstream reach is fed with water only (run 1), the resulting mobile-bed equilibrium slope will be considerably smaller than the upstream one.

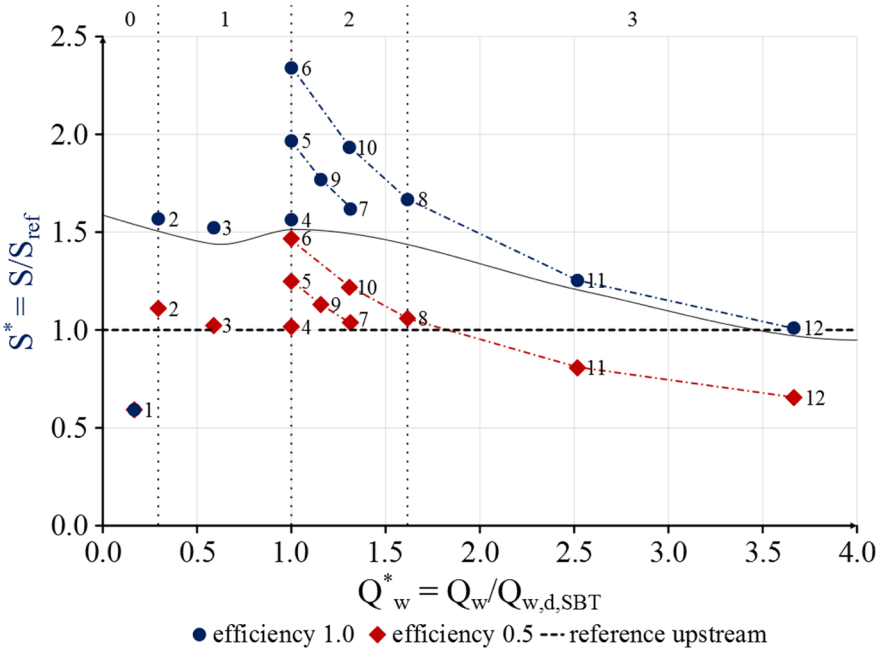

Figure 3: Results at mobile-bed equilibrium concerning riverbed slope represented by the non-dimensional slope S^*.

Another important finding is that the more water is released for a given sediment feeding rate (i.e. going from scenario 2 to scenario 3), the lower the resulting mobile-bed equilibrium slope (see the dot-dashed blue and red lines in Fig. 3), and the faster the mobile-bed equilibrium is reached. These results show that the final equilibrium configuration is dramatically dependent on the SBT-release scenario. Moreover, in the ideal case of e_{SBT} = 1.0, for each scenario in which the SBT is working (i.e. scenarios 1, 2, and 3, runs 2 to 12 in Fig. 3), the resulting riverbed slope is always higher than the upstream one.

4 Downstream morphological effects: preliminary results from field data analysis.

The Solis SBT was operated several times between 2012 (year of commissioning) and 2017, but only three operations delivered a significant amount of sediment-laden water to the downstream reach, i.e. the operation of August 13, 2014 and the two consecutive operations of June 11 and 16, 2016 (Müller-Hagmann 2017). Beside these operations, the others either delivered a negligible amount of sediment and water, or they did not last long enough to cause major changes to the downstream reach (Müller-Hagmann 2017).

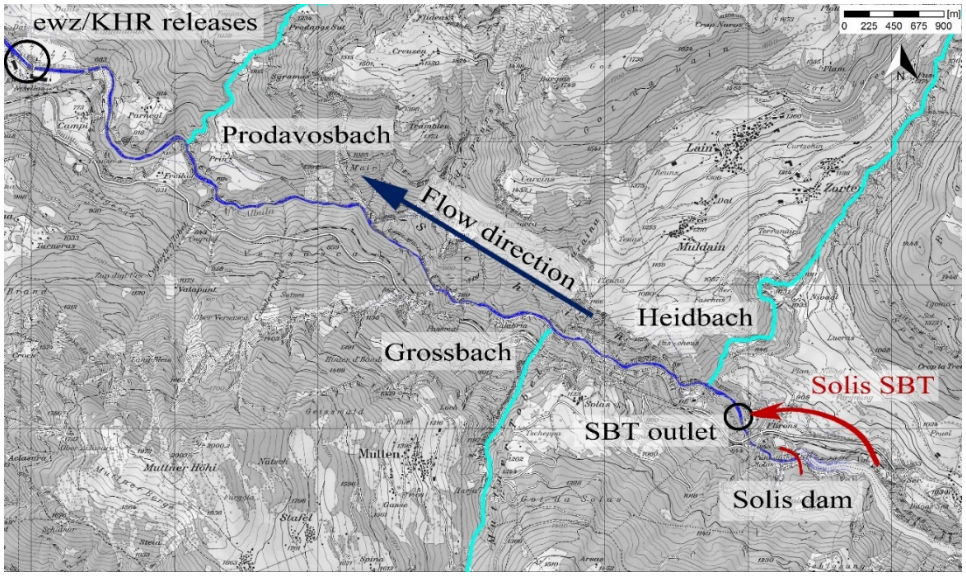

Figure 4: Plan view of Albula River between Solis dam and the intersection with the tailrace channel of the Sils hydropower plants of ewz (Elektrizitätswerk Zürich) and KHR (Kraftwerke Hinterrhein AG).

Two LiDAR surveys were performed at the Schin gorge along some 7 km downstream of the Solis dam and SBT outlet (Fig. 4) in October 2014 and October 2016, a few months after major SBT-operations. The point-clouds obtained from the LiDAR surveys have been classified to identify the measured points that are relative to buildings, vegetation, ground, and water. The identification of the water surface allows to correct the refraction-error related to the measurement of the riverbed. In fact, the performed LiDAR surveys take advantage of the use of a green laser that can penetrate the water surface and measure submerged riverbed points (e.g. Steinbacher *et al.* 2010). Then, a digital elevation model (DEM) is extrapolated from the classified point-cloud, and cross-section profiles are extracted from the DEM along the thalweg every ten meters. To estimate the changes in the cross-sectional areas, the same reference level is set below each cross-section. To minimize the error, each cross-section is cut ten meters above its lowest point (see cut level in Fig. 5), and the cross-sectional area is calculated as the area subtended from the cut cross-section (see Fig. 5).

During the operations of 2014 and 2016, the Solis SBT was operated with incoming water discharges smaller than the design discharge ($Q_{w,d,SBT}$ = 170 m^3/s, representing about a 5-year flood discharge), namely: Q_w = 153 m^3/s in 2014, and Q_w = 80 and 129 m^3/s in 2016. These values correspond to Q^*_w-values of 0.91 for 2014 and 0.48 and 0.76 for 2016. With $Q_{w,m,SBT}$ < 80 m^3/s all these releases belong to scenario 1 (see Fig. 1). We can compare the results of the numerical run with the field data analysis because the geometry used for the numerical study resembles the Albula, and the feeding GSD used for the runs is similar to the one sampled upstream of the Solis SBT. Based on the findings obtained from the numerical runs it is expected that both in the ideal case with e_{SBT} = 1.0, and in a more

realistic case with e_{SBT} = 0.5, for such values of Q^*_w, S^* is always above 1.0, i.e. $S > S_{ref}$ (Fig. 3). As the slope downstream of the Solis SBT is milder than the upstream one, we expect an increase in the downstream riverbed slope, i.e. aggradation is to be an expected outcome of 2014 and 2016 SBT releases at Solis. This is confirmed by the trend of cross-sectional area changes between 2014 and 2016 (see Fig. 6). Results presented in Fig. 6 are obtained comparing each cross-sectional area from the dataset of the two LiDAR surveys performed in October 2014 and 2016, after the 2014 and 2016 SBT operations, respectively. Since downstream of the confluence of the hydropower tailrace channel the Albula River is channelized, we plot the results relative to the first 7 km downstream of the Solis dam where the river results to be most prone to morphological changes (Fig. 4). The points relative to each cross-section are quite scattered, but the trend (dark blue solid line in Fig. 6) is clearly depositional.

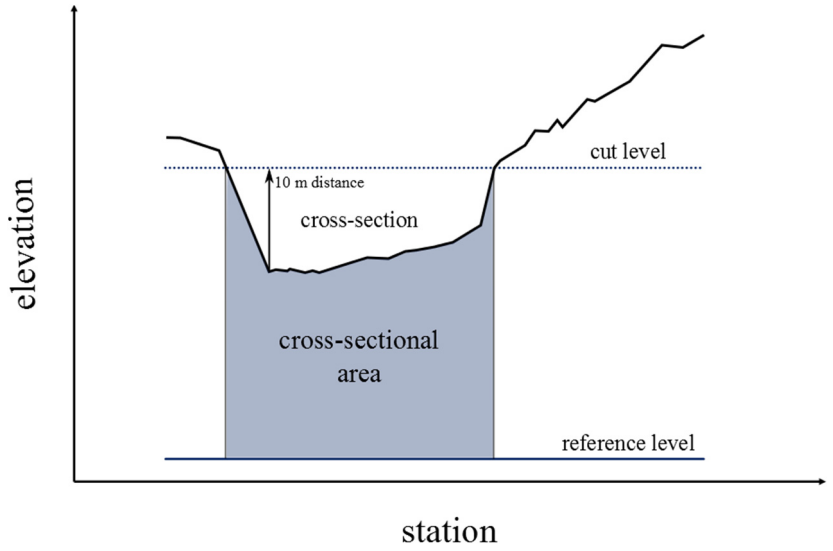

Figure 5: Sketch of a cross-section with reference level, the calculated area and the level at which each cross section is cut, i.e. ten meters above its lowest point.

5 Discussion and conclusions

A new concept for the identification of SBT-release scenarios has been developed and 1D numerical simulations have been performed to assess morphological changes caused by SBT releases. Numerical results have been verified against field data collected at the Albula River, precisely in the Schin gorge downstream of the Solis SBT. SBT-releases have the power to change riverbed slope and composition at mobile-bed equilibrium. Thereby, water and bedload discharges and bedload GSD delivered by the SBT play a major role, On the one hand, riverbed GSD approaches a static armor composition if only water is delivered from the SBT (scenario 0, $d^*_{s,g} > 6.0$). On the other hand, if an SBT is put in operation and delivers sediment-laden water to the downstream reach, the riverbed GSD approaches that of the feeding material, i.e. the riverbed becomes less armored with slight changes between different release conditions (scenarios 1, 2, and 3, $d^*_{s,g} \sim 1.5$).

Concerning riverbed slope, if no sediment is released, at mobile-bed equilibrium, the slope will be smaller than the upstream one (scenario 0, $S^* < 1$). Otherwise, at a fixed bedload feeding rate, the less water is released the steeper the riverbed becomes. While high bed slopes are a positive outcome for alpine stream morphology, since they favor the evolution of varied channel morphologies (i.e. step and pool, see e.g. Chin and Wohl 2005), an increase of the riverbed level caused by aggradation might raise the flooding danger. Eventually, halving the SBT-efficiency, i.e. the bedload discharge delivered by the SBT at a fixed water discharge, has small effects on the riverbed GSD, which becomes slightly coarser, while it has a larger impact on riverbed slope. In fact, there are several cases in which the slope is close to the upstream one (scenario 1 and some cases in scenario 2), and others in which the riverbed slope becomes smaller than the upstream one (for very large floods, i.e. scenario 3). While the SBT efficiency may thus be a mean to control riverbed aggradation if flooding becomes an issue in the downstream, a low efficiency would counteracts the reservoir desilting target of an SBT.

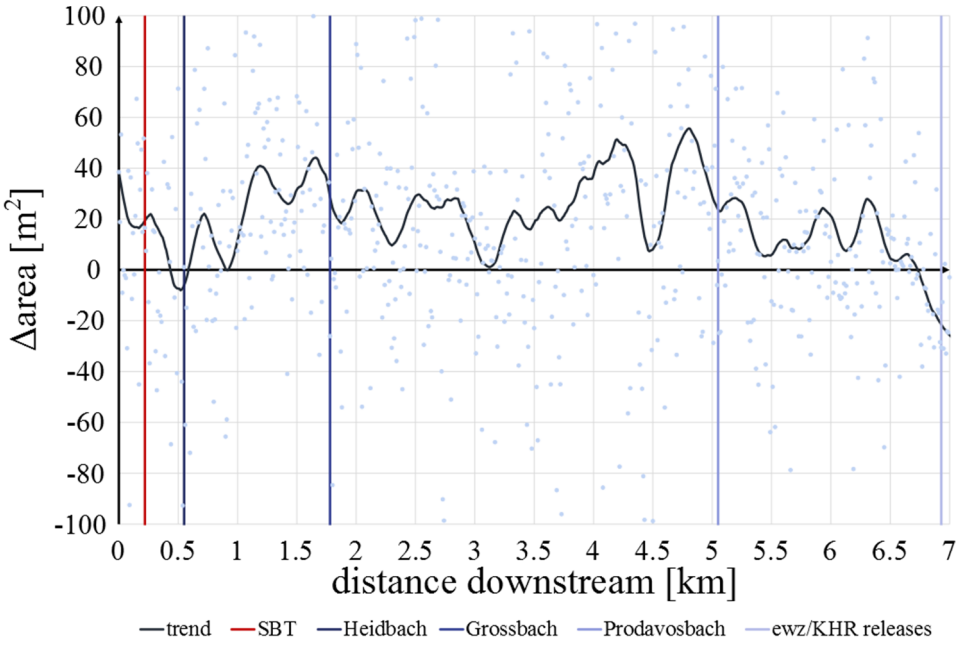

Figure 6: Cross-sectional changes between 2014 and 2016 (positive values represent deposition, negative values erosion); red vertical line represents the SBT outlet location, the other vertical lines represent major tributaries conjunctions; the dots represent single cross-sectional area changes (cross-sections are spaced along the river reach with a distance of 10 m) and the solid line represents the general trend (obtained with a zero-phase digital filtering of the scattered cross-sectional data).

Acknowledgements

The PhD project of the first author is financed by the Swiss Federal Office for the Environment (FOEN) in the “Hydraulic Engineering and Ecology” research program framework and is further affiliated to the Swiss Competence Center for Energy Research

– Supply of Electricity (SCCER-SoE). The authors would also like to thank Mr. Ziegler (ewz), Dr. Rickenmann (WSL), and Mrs. Müller-Hagmann (VAW) for providing data relative to the Solis SBT and dam operations, to the geometry of the upstream reach of the Albula River, and to water and sediment discharges in the Solis SBT, respectively.

References

Albayrak, I., Auel, C., Boes, R.M., and Müller-Hagmann, M. (2016), Mud Mountain Dam 9-foot Tunnel Re-armoring: Abrasion Calculations and Recommendations on the Invert Lining Concept, *Technical report*, Laboratory of Hydraulics, Hydrology and Glaciology (VAW), ETH, Zurich (unpublished).

Auel, C., Kantoush, S., and Sumi, T. (2016). Positive effects of reservoir sedimentation management on reservoir life - Examples from Japan. *Proc. 84th ICOLD Annual meeting* Johannesburg, South Africa**:** 4.11-14.20.

Boes, R.M., Beck, C., Lutz, N., Lais, A., and Albayrak, I. (2017). Hydraulics of water, air-water and sediment flow in downstream-controlled sediment bypass tunnels. *Proc. 2nd Intl. Workshop on Sediment Bypass Tunnels*, Kyoto, Japan.

Bunte, K. (2004). Gravel mitigation and augmentation below hydroelectric dams: a geomorphological perspective. *Report to the Stream Systems Technology Center*, USDA Forest Service, Fort Collins, USA.

Chin, A., and Wohl, E. (2005). Toward a theory for step pools in stream channels, *Progress in Physical Geography*, 29(3): 275–296

De Cesare, G., Manso, P., Daneshvari, M., and Schleiss, A.J. (2015). Laboratory research: Bed load guidance into sediment bypass tunnel inlet. *Proc. 1st Intl. Workshop on Sediment Bypass Tunnels*, Zurich, Switzerland: 169-179.

Facchini, M., Siviglia, A., and Boes, R.M. (2015). Downstream morphological impact of a sediment bypass tunnel – preliminary results and forthcoming actions. *Proc. 1st Intl. Workshop on Sediment Bypass Tunnels*, VAW-Mitteilungen 232 (R.M. Boes, ed.), ETH Zurich, Switzerland: 137-146.

Morris, G.L., and Fan, J. (1998). Reservoir Sedimentation Handbook: Design and Management of Dams, Reservoirs and Watersheds for Sustainable Use, McGraw-Hill Book Co., New York, USA.

Müller-Hagmann M. (2017). Hydroabrasion by sediment-laden high-speed flows in sediment bypass tunnels (tentative title). *VAW-Mitteilungen 239* (R. M. Boes, ed.), ETH Zurich, Switzerland: (in preparation).

Parker, G., and Sutherland, A.J. (1990). Fluvial armor. *Journal of Hydraulic Research*, 28(5): 529-544.

Robinson, C.T., Uehlinger, U., Monaghan, M.T. (2004). Stream ecosystem response to multiple experimental floods from a reservoir. *River Research and Applications*, 20(4): 359-377.

Schmidt, J.C., and Wilcock, P.R. (2008). Metrics for assessing the downstream effects of dams. W*ater Resources Research, 44(4)*: W04404.

Smart, G.M., and Jaeggi, M.N.R. (1983), Sediment Transport on Steep Slopes, *VAW-Mitteilungen 64* (D. Vischer, ed.), ETH Zurich, Switzerland.

Steinbacher, F., Pfennigbauer, M., Aufleger, M., Ullrich, A. (2010). AirborneHydroMapping – Area wide surveying of shallow water areas*. Proc. of 38th ISPRS Congres*, ISPRS.

Sumi, T., Okano, M., and Takata, Y. (2004). Reservoir sedimentation management with bypass tunnels in Japan. *Proc.9th Intl. Symposium on River Sedimentation,* Yichang, China: 1036-1043.

Vetsch, D., Siviglia, A., Ehrbar, D., Facchini, M., Kammerer, S., Koch, A., Peter, S., Vanzo, D., Vonwiller, L., Gerber, M., Volz, C., Farshi, D., Mueller, R., Rousselot, P., Veprek, R., Faeh, R. (2017). BASEMENT – Basic Simulation Environment for Computation of Environmental Flow and Natural Hazard Simulation. Version 2.7. © ETH Zurich, VAW.

Wilcock, P.R., and Crowe, J.C. (2003). Surface-based transport model for mixed-size sediment. *Journal of Hydraulic Engineering*, 129(2): 120–128.

Williams, G.P., and Wolman, M.G. (1984). Downstream effects of dams on alluvial rivers. *U.S. Geological Surveys Professional Papers*, 1286, US Geological Survey, Reston, USA.

Authors

Matteo Facchini (corresponding Author)
Annunziato Siviglia
Robert Michael Boes
Laboratory of Hydraulics, Hydrology and Glaciology, ETH Zurich, Switzerland
Email: facchini@vaw.baug.ethz.ch